

Thermodynamic consistency of liquid-gas lattice Boltzmann simulations

A. J. Wagner

Department of Physics, North Dakota State University, Fargo, North Dakota 58105, USA

(Received 5 July 2006; published 15 November 2006)

Lattice Boltzmann simulations have been very successful in simulating liquid-gas and other multiphase fluid systems. However, the underlying second-order analysis of the equation of motion has long been known to be insufficient to consistently derive the fourth-order terms that are necessary to represent an extended interface. These same terms are also responsible for thermodynamic consistency—i.e., to obtain a true equilibrium solution with both a constant chemical potential and a constant pressure. In this article we present an equilibrium analysis of nonideal lattice Boltzmann methods of sufficient order to identify those higher-order terms that lead to a lack of thermodynamic consistency. We then introduce a thermodynamically consistent forcing method.

DOI: [10.1103/PhysRevE.74.056703](https://doi.org/10.1103/PhysRevE.74.056703)

PACS number(s): 47.11.-j, 47.10.-g, 47.55.Ca

I. INTRODUCTION

The standard lattice Boltzmann approach leads to an ideal-gas equation of state. Several different approaches to simulate nonideal fluids with lattice Boltzmann have been introduced in the past. The main application has been to simulate phase separation, although other applications like an increase in the speed of sound have also been considered. There are two different philosophies to introduce the nonideal terms. The first is guided by an atomistic picture, and local interactions are introduced through a forcing term [1,2]. The second starts from the Navier-Stokes equation for a nonideal gas and tries to match the hydrodynamic limit of the lattice Boltzmann equation with this macroscopic equation [3,4]. An analysis of these different models up to second order is given by Aurell and Do-Quang [5].

Whatever the underlying philosophy, each approach leads to some nonideal equation of state. Knowing the equation of state is sufficient to predict the phase behavior from equilibrium thermodynamic arguments. The equilibrium densities are determined through the Maxwell construction [6]. Many approaches fail this test, and the resulting phase diagrams deviate from the theoretical one. There is one brilliant analysis of the failure of the Shan-Chen model to recover thermodynamic equilibrium by Shan and Chen themselves [2]. Other authors have remained quiet on the subject.

For many simple applications where phase separation is only required to form a nearly immiscible system, these thermodynamic details may be of limited importance. For simulations of phase separation, however, such details can be crucial. In this paper we will examine why lattice Boltzmann approaches using a force to introduce the nonideal equation of state fail to obtain the correct thermodynamic behavior. We explicitly identify the terms that lead to the nonthermodynamic behavior of these methods.

The paper is organized as follows: we first identify the hydrodynamic equations that we intend to simulate. We then discuss the equilibrium behavior of these equations. We then introduce a general lattice Boltzmann method which introduces nonideal terms through either forcing or pressure terms. The hydrodynamic limit of this approach is presented. This allows us to identify how we can incorporate the non-

ideal pressure contributions by either incorporating a bulk force or by altering the pressure moment of the equilibrium distribution.

These two different methods for nonideal systems are equivalent to the method of Chen *et al.* [4] or the more recent extension by He *et al.* [7,8] when we use the bulk force and the Holdych correction to the Swift model [9] when we directly alter the pressure moment. However, we are not able to consistently introduce surface tension effects at this point since those appear as higher-order derivatives that are not derivable by a second-order expansion [10].

These higher-order derivatives, however, are necessary to achieve thermodynamic consistency. We introduce a near-equilibrium analysis of sufficient order to consistently derive these higher-order gradient terms. This analysis uncovers correction terms for pressure and forcing methods. Despite the fact that we only perform a fifth-order analysis we are able to identify the correction terms exactly when the fluid is not advected with respect to the lattice. With this knowledge we are then able to formulate a forcing method that achieves thermodynamic consistency.

II. EQUATIONS OF MOTION FOR A NONIDEAL GAS

As a simple example of a nonideal fluid we will examine a single-component fluid that can undergo a liquid-gas phase transition. For simplicity an isothermal system is considered. Such a system has an underlying free energy of the form

$$F = \int [f(\rho) + I(\nabla\rho, \nabla^2\rho, \dots)] dx, \quad (1)$$

where ρ is the density, $f(\rho)$ is the bulk free energy, and $I(\nabla\rho, \nabla^2\rho, \dots)$ is a gradient expansion of the interfacial free energy. The lowest-order term for the free energy is $\frac{\kappa}{2}(\nabla\rho)^2$, and usually only this term is considered. The equations of motion for a nonideal gas are given by the continuity equation

$$\partial_t\rho + \nabla(\rho\hat{\mathbf{u}}) = 0, \quad (2)$$

where $\hat{\mathbf{u}}$ is the velocity of the fluid and the Navier-Stokes equation of a nonideal gas,

$$\rho \partial_t \hat{\mathbf{u}} + \rho \hat{\mathbf{u}} \cdot \nabla \hat{\mathbf{u}} = \rho \nabla \mu + \nabla \sigma. \quad (3)$$

Here $\mu = \frac{\partial F}{\partial \rho}$ is the chemical potential of the nonideal gas and $\sigma = \nabla \hat{\mathbf{u}} + (\nabla \hat{\mathbf{u}})^T - \frac{2}{3} \nabla \cdot \hat{\mathbf{u}} \mathbf{1}$ is the Newtonian stress tensor.

Let us consider how this system will approach equilibrium. The equilibrium will be time independent, and the flow will be uniform—i.e., $\hat{\mathbf{u}} = \text{const.}$ So Eq. (3) reduces to

$$\nabla \mu = 0, \quad (4)$$

so that the chemical potential will be constant in equilibrium.

Condition (4) only guarantees that the chemical potential is constant in both phases. Bulk thermodynamics, however, requires that the pressure be also constant in equilibrium. This is guaranteed through the thermodynamic relation

$$\rho \nabla \mu = \nabla P, \quad (5)$$

where P is the pressure tensor. This pressure tensor is defined through the properties that it is equal to the bulk pressure in the absence of density gradients $P = p \mathbf{1} = [\rho \partial_\rho f(\rho) - f(\rho)] \mathbf{1}$ and through condition (5) in the interfacial areas [11]. With this relation a uniform chemical potential is equivalent to a divergence-free pressure tensor.

As an aside it is interesting to note that this statement is more general than bulk thermodynamics. It can even be applied to finite systems with curved interfaces. An example is an equilibrium drop that will have a constant chemical potential, but the pressure inside the drop will differ from the pressure outside by the Laplace pressure $\Delta p = \frac{\sigma}{\rho}$, where σ is the surface tension. Despite this difference in the pressures inside and outside the drop, the divergence of the pressure tensor vanishes everywhere. For such a system with a curved interface the equilibrium liquid and gas densities will differ slightly from the bulk thermodynamic values [12].

The connection between bulk thermodynamics and the equilibrium condition $\rho \nabla \mu = \nabla P = 0$ can be established by considering a flat interface between the liquid and gas phases. Assume that this interface is orthogonal to the x axis. In this case $\nabla P = \partial_x P_{xx} \mathbf{e}_x$ is just the derivative of a scalar function. Therefore it follows from $\nabla P = 0$ that in the bulk phase $p_l = p_g$. Therefore the solution of the differential equation $\nabla P = \rho \nabla \mu = 0$ for a flat interface implies the standard bulk thermodynamic equilibrium conditions $\mu_l = \mu_g$ and $p_l = p_g$.

Let us consider the condition $\rho \nabla \mu = 0$ in some more detail. For concreteness' sake let us assume that $I(\nabla \rho, \dots) = \frac{\kappa}{2} (\nabla \rho)^2$. We then obtain $\mu = \partial_\rho f(\rho) - \kappa \nabla^2 \rho$ and $P = [\rho \partial_\rho f(\rho) - f(\rho) - \kappa \rho \nabla^2 \rho - (\kappa/2) (\nabla \rho)^2] \mathbf{1} + \kappa \nabla \rho \nabla \rho$. Then the differential equation for a single flat interface becomes

$$\kappa \partial_x^3 \rho = \partial_x \partial_\rho f(\rho), \quad (6)$$

subject to the boundary conditions that

$$\lim_{x \rightarrow \pm\infty} \partial_x \rho = 0. \quad (7)$$

Because Eq. (6) is equivalent to both $\nabla \mu = 0$, and $\nabla P = 0$, the limiting values for the density will be the equilibrium densities ρ_g and ρ_l . This conclusion, however, is independent of the form of the interfacial energy term $I(\nabla \rho, \nabla^2 \rho, \dots)$, and as long as the new differential equation has a solution that ful-

fills the boundary condition (7), the limiting densities ρ_g and ρ_l will be the same.

The important corollary of this argument is that while there are many possible forms of the chemical potential and corresponding pressure tensor that lead to the correct bulk phase behavior, arbitrary derivative terms (which might arise because of unintentional higher-order corrections to the numerical method) will in general not be derivable from an interfacial energy term $I(\nabla \rho, \dots)$. In such a situation the differential equation (4) can lead to bulk densities that do not correspond to the equilibrium densities. These situations are the main concern of this paper.

III. LATTICE BOLTZMANN METHOD

The lattice Boltzmann method can be viewed as a discretization of the Boltzmann equation. And in the same way that the Boltzmann equation describes a gas that at long wavelength obeys the hydrodynamic equations, the same is true for the lattice Boltzmann method. In the lattice Boltzmann method both the space and velocity space are discretized and the basic variables are the densities $f_i(x, t)$ associated with the velocity v_i . The hydrodynamic variables are then the local density

$$\rho(x, t) = \sum_i f_i(x, t) \quad (8)$$

and the momentum

$$\rho(x, t) \mathbf{u}(x, t) = \sum_i f_i(x, t) \mathbf{v}_i. \quad (9)$$

Most lattice Boltzmann methods do not conserve energy and instead enforce a constant temperature. A remarkable model that includes energy conservation for a fluid with an ideal gas equation of state has recently been presented by Ansumali and Karlin [13]. For fluids with a nonideal equation of state, however, no satisfactory models have been developed to date. One caveat is that \mathbf{u} is not necessarily the local velocity, as we will see below.

The evolution equation for a nonideal fluid can be written as

$$f_i(\mathbf{x} + \mathbf{v}_i, t + 1) = f_i(\mathbf{x}, t) + F_i(\mathbf{x}, t) + \frac{1}{\tau} [f_i^0(\rho) + A_i(\mathbf{x}, t) - f_i(\mathbf{x}, t)]. \quad (10)$$

Here f_i^0 is the equilibrium distribution for the ideal gas. The A_i represent nonideal contributions to the pressure tensor [3], and F_i are contributions of an external force. The force can also be used to mimic interactions in a mean-field manner.

In the lattice Boltzmann method the Navier-Stokes equations are not discretized directly; instead, the moments of the equilibrium distribution as well as A_i and F_i are chosen such that the momentum moment of a second-order expansion of the lattice Boltzmann equation will give the desired Navier-Stokes equation (3). A dilemma occurs when the pressure tensor itself contains second-order derivative terms since these terms are formally higher than second order in the Navier-Stokes equations. These terms are not consistently

derived in standard lattice Boltzmann expansion techniques.

So the question arises: how can these terms be consistently incorporated into a lattice Boltzmann method? One may consider simply expanding the lattice Boltzmann equation to higher order, but this will lead to Burnett level equations, which is not the desired result. The reason that these higher-order density derivatives appear in the Navier-Stokes equation is because the density derivatives are not small near an interface and these terms are responsible for the surface tension.

It is difficult and rather cumbersome to extend the expansion of the lattice Boltzmann equation to higher orders in a general way. So instead we will consider an equilibrium (or at least stationary state) interface instead and develop a higher-order analysis for this situation. Doing so uncovers the additional terms that lead to a lack of thermodynamic consistency for forcing methods. Incorporating these terms allows for thermodynamic consistency as will be discussed below.

There are two expansion methods that are regularly used to derive the hydrodynamic limit of the lattice Boltzmann equations: they are referred to as the Taylor expansion and the Chapman-Enskog methods. Up to second order the methods give identical results, but there is debate about the equivalence of the two methods for higher-order results [14]. In this paper we will utilize the first method.

To establish a starting point for a higher-order expansion we will first present the standard second-order expansion. We will then show how to choose the moments of f_i^0 , A_i , and F_i to simulate a van der Waals gas.

IV. SECOND-ORDER EXPANSION

To obtain the hydrodynamic equations that govern the evolution of the slow dynamics of the conserved quantities we use a Taylor expansion of Eq. (10) to second order. As usual we will only conserve mass, defined through the density (8) and momentum defined through (9).

For this isothermal model, which does not include a conserved energy moment, we require knowledge of the first three velocity moments of the equilibrium distribution function. These are given by

$$\sum_i f_i^0 = \rho, \quad (11)$$

$$\sum_i f_i^0 (\mathbf{v}_i - \mathbf{u}) = 0, \quad (12)$$

$$\sum_i f_i^0 (\mathbf{v}_i - \mathbf{u})(\mathbf{v}_i - \mathbf{u}) = \rho \theta \mathbf{1}, \quad (13)$$

$$\sum_i f_i^0 (v_{i\alpha} - u_\alpha)(v_{i\beta} - u_\beta)(v_{i\gamma} - u_\gamma) = Q_{\alpha\beta\gamma}. \quad (14)$$

Galilean invariance would require the third-order tensor Q to vanish. In most standard lattice Boltzmann methods this term does not vanish, however, because these models contain too small a velocity set. For these models $v_{ix}^3 = v_{ix}$, which pre-

cludes the presence of the third power of \mathbf{u} in the $\sum_i f_i^0 v_{ix}^3$ moment. It also fixes the temperature to be $\theta = \frac{1}{3}$. Therefore most models have a Q term given by the third-order tensor $Q = \rho \mathbf{u} \mathbf{u} \mathbf{u}$. The effects of the Galilean invariance violation caused by this term become noticeable only at large velocities \mathbf{u} [15].

The nonideal contributions from the A_i need to conserve mass and momentum, and the moments are given by

$$\sum_i A_i^0 = 0, \quad (15)$$

$$\sum_i A_i^0 (\mathbf{v}_i - \mathbf{u}) = 0, \quad (16)$$

$$\sum_i A_i^0 (\mathbf{v}_{i\alpha} - \mathbf{u}_\beta)(\mathbf{v}_{i\beta} - \mathbf{u}_\beta) = A_{\alpha\beta}, \quad (17)$$

$$\sum_i A_i^0 (v_{i\alpha} - u_\alpha)(v_{i\beta} - u_\beta)(v_{i\gamma} - u_\gamma) = A_{\alpha\beta\mu\gamma} + A_{\alpha\gamma\mu\beta} + A_{\beta\gamma\mu\alpha}. \quad (18)$$

The forcing term F_i needs to conserve mass; therefore,

$$\sum_i F_i = 0. \quad (19)$$

It also needs to change the momentum by an amount \mathbf{F} ; therefore, we choose

$$\sum_i F_i (\mathbf{v}_i - \mathbf{u}) = \mathbf{F}. \quad (20)$$

The second moment of the forcing term is usually taken to be zero, but we leave a general term Ψ which we will use later to contain a correction term:

$$\sum_i F_i (\mathbf{v}_i - \mathbf{u})(\mathbf{v}_i - \mathbf{u}) = \Psi. \quad (21)$$

At this point it is worthwhile to note that the distinction between the A and Ψ terms is somewhat artificial. Both terms enter the lattice Boltzmann equation in the same way, so that instead of Ψ , we can insert the term $A = \tau\Psi$ and vice versa. We distinguish between these terms to connect our analysis to established methods. Pressure methods [3,9] only use A and forcing methods [4,7,8,10,16] only F and Ψ .

Now we need to derive the hydrodynamic limit of the lattice Boltzmann equation (10) to link this method to the hydrodynamic equations (2) and (3) which we want to simulate.

A. Hydrodynamic limit

While the Taylor expansion method is in principle well known, we will present it here again because the higher-order analysis presented later in this paper uses the results and techniques of this approach. The main premise of the Taylor expansion approach is that the distribution function can be expressed by a Taylor expansion

$$f_i(x + v_i \Delta t, t + \Delta t) = \sum_k \frac{(\Delta t)^k}{k!} D^k f_i(x, t), \quad (22)$$

where we have defined the derivative operator $D_i = (\partial_t + v_i \nabla)$. For this expansion to be useful we must make the assumption that derivatives are small. One could phrase the same argument in terms of Δt , but it will be convenient to set $\Delta t = 1$ in Eq. (10). To order our terms we will therefore use the derivatives as a small parameter ϵ so that $O(\partial^n) = O(\epsilon^n)$. We obtain, for Eq. (10) to second order,

$$D_i f_i + \frac{1}{2} D_i^2 f_i + F_i + O(D^3) = \frac{1}{\tau} (\hat{f}_i^0 - f_i), \quad (23)$$

where we have introduced $\hat{f}_i^0 = f_i^0 + A_i$. This relates nonlocal f_i to local f_i and their derivatives. However, the f_i remain unknown and we only know the \hat{f}_i^0 in terms of the macroscopic quantities. We can use Eq. (23) to express f_i in terms of the equilibrium distribution and higher-order derivatives:

$$f_i = \hat{f}_i^0 - \tau F_i - \tau D_i f_i + O(\partial^2) = \hat{f}_i^0 - \tau F_i - \tau D_i (\hat{f}_i^0 - \tau F_i) + O(\partial^2). \quad (24)$$

Using this approximation we can now express the lattice Boltzmann equation purely as a differential equation in terms of the equilibrium distribution and the collision term:

$$F_i + D_i (\hat{f}_i^0 - \tau F_i) - \left(\tau - \frac{1}{2} \right) D_i^2 (\hat{f}_i^0 - \tau F_i) = \frac{1}{\tau} (\hat{f}_i^0 - f_i) + O(\partial^3). \quad (25)$$

Taking the zeroth-order velocity moment Σ_i , Eq. (25), we obtain [borrowing the Euler level terms—i.e., the terms of $O(\partial)$ —of the momentum equation (29)] the continuity equation

$$\partial_t \rho + \nabla \cdot \left(\rho \mathbf{u} - \frac{1}{2} \mathbf{F} \right) = O(\partial^3). \quad (26)$$

This leads us to identify the mean fluid velocity as

$$\hat{\mathbf{u}} = \mathbf{u} - \frac{1}{2\rho} \mathbf{F}. \quad (27)$$

We then obtain the continuity equation

$$\partial_t \rho + \nabla \cdot (\rho \hat{\mathbf{u}}) = O(\partial^3). \quad (28)$$

Taking the first-order velocity moment $\Sigma_i v_i$, Eq. (25), we obtain the Navier-Stokes level equation

$$\rho \partial_t \hat{\mathbf{u}} + \rho \hat{\mathbf{u}} \cdot \nabla \hat{\mathbf{u}} = -\nabla(\rho \theta + A) + F + \nabla \sigma + \nabla R + O(\partial^3), \quad (29)$$

where the Newtonian stress tensor σ is given by

$$\sigma = \nu \rho [\nabla \hat{\mathbf{u}} + (\nabla \hat{\mathbf{u}})^T] \quad (30)$$

and unphysical terms have been collected in the remainder tensor

$$R = \tau \Psi - 3\nu [\hat{\mathbf{u}} \nabla \cdot A + (\hat{\mathbf{u}} \nabla \cdot A)^T + \hat{\mathbf{u}} \cdot \nabla A \mathbf{1} + \nabla Q] + O(\partial^2). \quad (31)$$

The kinematic viscosity is given by $\nu = (\tau - \frac{1}{2})\theta$. Note that while we wrote $\hat{\mathbf{u}}$ in Eqs. (30) and (31) it cannot be distinguished from \mathbf{u} here because the forcing term is $O(\partial)$ and therefore $\hat{\mathbf{u}} = \mathbf{u} + O(\partial)$. We also note that most of the unphysical terms in Eq. (31) violate Galilean invariance [9,15].

B. Forcing and pressure methods for the nonideal gas

If we set both A and F to zero, we obtain the, Navier-Stokes equation for an ideal gas. To obtain the Navier Stokes equation for a nonideal gas previous research has identified two different strategies. One option is to use the forcing term to introduce the nonideal contribution to the equation of state [4]. The form presented here was first presented in the elegant work of He *et al.* [7,8]. In this case, which we will refer to as the forcing method, we define

$$\begin{aligned} F &= -\nabla \cdot P^{nid}, \\ \Psi &= 0, \\ A &= 0, \end{aligned} \quad (32)$$

where $P^{nid} = P - n\theta \mathbf{1}$ is the nonideal part of the pressure tensor. The second approach is based on the idea of including the nonideal pressure in the second moment of the equilibrium distribution [3,9]. To do this we define

$$\begin{aligned} F &= 0, \\ \Psi &= 0, \end{aligned}$$

$$A = P - \rho \theta \mathbf{1} + \nu (\hat{\mathbf{u}} \cdot \nabla \rho + (\hat{\mathbf{u}} \cdot \nabla \rho)^T + \hat{\mathbf{u}} \cdot \nabla \rho \theta \mathbf{1}), \quad (33)$$

where the ν terms have been introduced by Holdych *et al.* [9] and later by Inamuro *et al.* [17]. To do this we have to use the near-equilibrium approximation of $A = -\rho \theta + O(\epsilon)$, as discussed by Kalarakis [18].

Up to second order in the derivatives both of these approaches lead to the same hydrodynamic equations

$$\partial_t \rho + \nabla \cdot (\rho \hat{\mathbf{u}}) = 0, \quad (34)$$

$$\rho \partial_t \hat{\mathbf{u}} + \rho \hat{\mathbf{u}} \cdot \nabla \hat{\mathbf{u}} = -\nabla P + \nabla \sigma. \quad (35)$$

For the van der Waals pressure for a critical density of 1 and a temperature $\theta = \frac{1}{3}$ the pressure tensor is given by

$$P = \left(\frac{\rho}{3 - \rho} - \frac{9}{8} \rho^2 \theta_c \right) \mathbf{1}. \quad (36)$$

Using this pressure for the two methods we observe phase separation below the critical temperature as shown in Fig. 1. There are, however, a number of peculiarities.

Let us first discuss the results for the pressure method. There is no unique solution. Three different profiles for the pressure method are shown in Fig. 1(a). All of them are

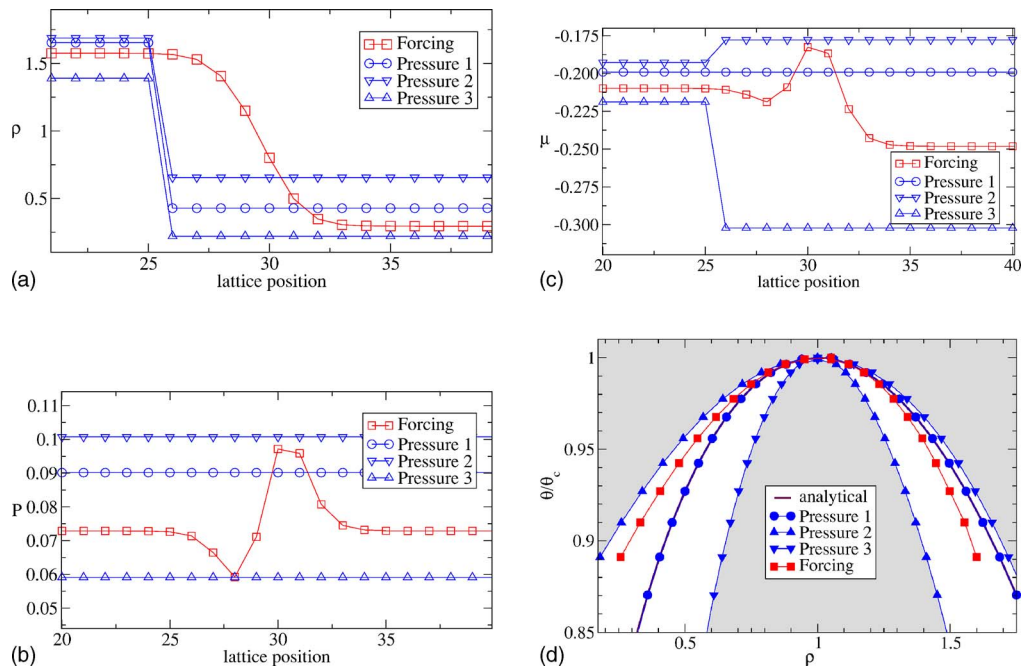


FIG. 1. (Color online) Comparison of the profile (a) and the phase diagram (b) for the van der Waals pressure of Eq. (36) obtained by the forcing method of Eq. (32) with the pressure method from Eq. (33). There is no unique solution to the pressure method. The unique solution of the forcing method is not in agreement with the theoretical phase diagram. The critical temperature used in (a)–(c) was $\theta_c = 0.37$ at a temperature of $\theta = 1/3$. In (d) no liquid-gas phase boundaries can lie outside the white area and still have equal pressures for the liquid and gas phase.

stable solutions which are stable against small perturbations. Also the density profiles are sharp, switching from the liquid to the gas density in only one lattice spacing. These profiles correspond to a constant-pressure profile [Fig. 1(b)], which is exact to machine accuracy. The chemical potential profiles, however, are vastly different as shown in Fig. 1(c). Only the middle profile corresponds to a constant chemical potential and therefore to the thermodynamic equilibrium. In Fig. 1(d) we show the phase diagrams. Only in the white area in this diagram can liquid and gas phases have equal pressures. We show the results of simulations which are initialized with a near-constant pressure in the gas and liquid phases. The Δ triangles correspond to simulations initialized with the lowest possible constant pressure, and the ∇ triangles correspond to simulations initialized with the highest possible constant pressure. All these simulations are stable to small perturbations. It appears that all states with equal pressures, including but not limited to the true equilibrium state, are stable solutions.

The forcing method leads to a unique profile which has an interface extending over several lattice spacings. The bulk pressures of the liquid and gas phases agree, but there are variations of the pressure (36) around the interface in Fig. 1(b). The bulk values of the chemical potential, however, are not equal. It is therefore not surprising that the phase diagram differs from the true equilibrium profile as shown in Fig. 1(d).

To understand these results let us recall that expression for the pressure, Eq. (36), does not contain any gradient terms. This corresponds to $I(\nabla\rho, \nabla^2\rho, \dots) = 0$ in the expression for the free energy, Eq. (1). This means that we have not input

any interfacial free energy contributions, and we therefore expect a sharp interface. But without interfacial contributions the differential equation $\nabla P = 0$ is no longer a differential equation. Instead this only requires that the pressure for both phases be the same, $p_l = p_g$. Any such pressures will fulfill $\nabla P = 0$, as shown in Fig. 1(b). In this figure numerical solutions at the maximum and minimum of the coexistence liquid and gas pressures as well as the true equilibrium pressure are shown. Only for the true equilibrium densities will $\mu_l = \mu_g$ be true as can be seen in Fig. 1(c). So clearly $\nabla P = \rho \nabla \mu$ is no longer generally valid. There is no guarantee that a system without interfacial energy obeying the dynamic equations (2) and (3) will move towards true equilibrium. This explains why the pressure method, which leads to the expected sharp interface, can fail to recover the equilibrium densities.

This, however, is not enough to understand the stability of the interfaces to small perturbations. To change the liquid and gas densities it is in general necessary to move the interface. Because the method leads to a sharp interface, moving this interface will lead to states that have one lattice point with a density between the gas and liquid densities. If the gas density is slightly increased, the pressure will also increase, favoring a return to the original density. Likewise, if at one point the liquid density is reduced, this will lead to a lower pressure inducing the return to the original density commensurate with the surrounding pressure. So the stability of these nonequilibrium structures occurs because moving an interface requires different discretizations of the interface. And these discretizations lead to position-dependent pressures which counteract the movement of the interface.

The results shown in Fig. 1 are at a mean velocity of zero. The situation changes when a mean velocity is added to the

system. In these cases we do not find advected stationary solutions, but instead large oscillations are observed for sharp interfaces. This violation of Galilean invariance is removed by increasing the width of the interface, as shown in [15].

In the case of the forcing method the situation is more complicated. The forcing method leads to a unique extended interface as shown in Fig. 1(a). Since we do not obtain a sharp interface, the pressure P of Eq. (36) is not constant, as seen in Fig. 1(b). Therefore higher-order gradient terms must be present in the pressure for this lattice Boltzmann method. These gradient terms arise because of higher-order terms in the lattice Boltzmann method that were not picked up by our second-order expansion. The bulk values of the pressure in Fig. 1(b) are the same for the liquid and gas phases as is to be expected from the condition of mechanical equilibrium. The same, however, is not true for the chemical potential in Fig. 1(c). Because the bulk values of the chemical potential are not the same, the densities also do not correspond to their equilibrium values.

For the pressure method there are two potential remedies for us to recover the equilibrium bulk densities for the liquid and gas phases. The most obvious one, in light of the present discussion, is to explicitly include the correct gradient terms in the pressure, and we will follow that route below. A second potential remedy lies in including fluctuation terms in the Navier-Stokes equations. Incorporating equilibrium fluctuations allows the interfaces to move and to select the correct equilibrium bulk densities for the pressure method. This approach, however, is outside the scope of the current paper.

While derivatives in the pressure tensor are not consistent with the second-order expansion, it appears reasonable to include the full derivative terms in the pressure tensor. This is indeed what was done in the original pressure method [3], and since the numerical simulations do not indicate the presence of any spurious interfacial terms, it is not surprising that this approach is successful for the pressure algorithm.

The usefulness of including the full gradient terms in the pressure tensor is less obvious for the forcing method where there are clearly already significant, spurious interfacial terms present that lead to an extended interface.

So we will now replace Eq. (36) with

$$P = \left[\frac{\rho}{3 - \rho} - \frac{9}{8} \rho^2 \theta_c - \kappa \left(\rho \nabla^2 \rho + \frac{1}{2} \nabla \rho \cdot \nabla \rho \right) \right] \mathbf{1} + \kappa \nabla \rho \nabla \rho. \quad (37)$$

For a numerical implementation the gradient and Laplace operator have to be replaced by discrete versions. This is problematic because it will in general break the relation $\nabla P = \rho \nabla \mu$ and, thereby, also the exact thermodynamic consistency. For interfaces that are wide enough, though, this relation will still hold to good approximation. We have not yet been able to identify a discrete derivative operator and an expression for the pressure that preserves $\nabla^D P = \rho \nabla^D \mu$. Such an expression could guarantee that a constant pressure is exactly equivalent to a constant chemical potential, and therefore it would exactly recover equilibrium thermodynamics.

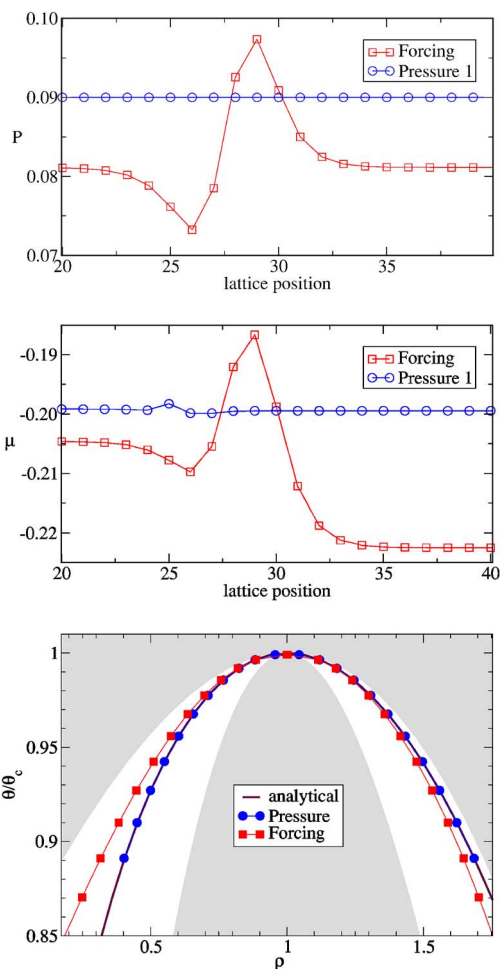


FIG. 2. (Color online) The phase behavior for a liquid gas system when the explicit interfacial energy is included. For this set of simulations we used $\kappa=0.1$ in the expression for the pressure, Eq. (37). All other parameters are the same as for Fig. 1.

For the simulations presented in this paper we require the one-dimensional discrete gradient and Laplace operator. We use the discretization

$$\nabla^{(D)} f(x) = \frac{1}{2} [f(x+1) - f(x-1)], \quad (38)$$

$$\nabla^{2(D)} f(x) = f(x+1) - 2f(x) + f(x-1). \quad (39)$$

For $\kappa=0$ expression (37) leads to Eq. (36). But for finite κ we now expect to find an extended interface for the pressure method. We also expect that a constant pressure will now reduce the difference in the chemical potential for the two phases. The results are shown in Fig. 2.

For a sufficiently large interfacial energy contribution of $\kappa=0.1$ there is now a unique solution for the pressure method. This solution also agrees very well with the analytical phase diagram. We find that the pressure is constant up to machine accuracy and the chemical potential is very nearly constant. In particular the deviation in the bulk value of the chemical potential in the gas and liquid phases is less than 3×10^{-4} .

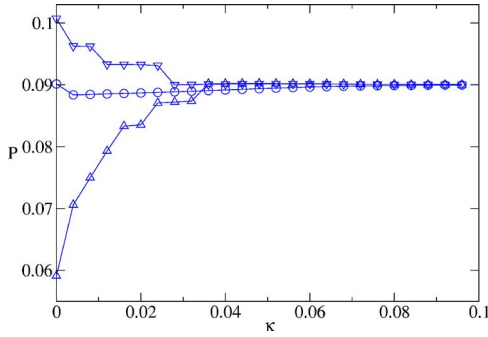


FIG. 3. (Color online) Convergence of the pressure in the two-phase system for different initial conditions for $\theta=0.37$. A unique solution is only found for large enough values of κ . For a detailed discussion of this effect see the main text.

In the continuous situation the nondefiniteness of the stationary state is limited strictly to $\kappa=0$. For a discrete approach $\nabla^D P = \rho \nabla^D \mu$ is not generally valid, and therefore it is not *a priori* clear that an arbitrarily small interfacial term in the pressure will guarantee a convergence to the equilibrium solution. As we have seen before it is not even guaranteed that it will converge to a unique solution. We therefore performed a set of simulations for different values of κ from 0 to 0.1 with initial conditions that correspond to extreme values of the equal pressure as well as the equilibrium solution. The simulation results are shown in Fig. 3. We see that nonuniqueness survives for finite κ . The range of possible pressures is rapidly reduced until a near-unique solution is found at κ larger than about 0.08.

The origin of this nonuniqueness even in the presence of an interfacial energy lies in the discretization of the interface. Moving the interface over the lattice requires a re-discretization of the interface. Each of these discretizations will have a different interfacial free energy $\Sigma_i(\kappa/2)(\nabla \rho)^2$. To visualize this imagine a sharp interface of Fig. 1(a). This interface has only two points with nonvanishing gradient and Laplace operators. If this interface moves, there will have to be at least one point with intermediate value of ρ and now there are at least three points with nonvanishing gradient and Laplace terms. Therefore moving the interface will change the total free energy. Mass conservation generally implies that changing the liquid and gas densities requires changing the relative gas and liquid volumina. Therefore changing the densities requires that the interfaces move. But if moving the interface requires passing a local maximum in the free energy, this implies that the system is at least in a metastable state. And a lattice Boltzmann method without fluctuations cannot escape such a metastable state. So to move an interface that is well aligned with the lattice one has to overcome a free energy barrier with respect to the less favorable discretization of the interface and the simulation can get stuck in a nonequilibrium configuration.

The forcing method is also noticeably improved through the inclusion of the gradient terms. The difference in the bulk chemical potential is about halved from 0.03 to 0.015. This is still about 50 times larger than the difference for the pressure method. This difference in the chemical potential translates to a deviation of the liquid and gas densities from their equi-

librium values. This can be clearly seen in Fig. 2(d). In order to understand the origin of the large deviations of the forcing method from the thermodynamic equilibrium we need to uncover the spurious gradient terms in the effective pressure. To do this we need to improve our expansion method to consistently derive those derivative terms.

V. HIGHER-ORDER NEAR-EQUILIBRIUM EXPANSION

To identify the higher-order terms of the equilibrium structure we perform a fifth-order expansion around an equilibrium profile which is stationary, but possibly advected with a constant velocity U . As before we make the assumption that derivatives are small [$O(\partial)=O(\epsilon)$]. From Eq. (29) we already know that $O(F)=O(\partial)=O(\epsilon)$. To avoid obtaining too many terms we will limit our analysis here to small velocities, so we also postulate $O(U)=O(\epsilon)$. Note that since we will only neglect terms of order $O(\epsilon^5)$, we will not lose any of the terms present in the lower-order expansion, with the single exception of the $\nabla^2 Q$ term in Eq. (30).

Performing a Taylor expansion to fifth order in the derivatives of Eq. (10) and expressing the f_i in terms of $\hat{f}_i^0 = f_i^0 + A_i$ we obtain

$$\begin{aligned} F_i + D(\hat{f}_i^0 - \tau F_i) - \left(\tau - \frac{1}{2} \right) D^2(\hat{f}_i^0 - \tau F_i) + \left(\tau^2 - \tau + \frac{1}{6} \right) \\ \times D^3(\hat{f}_i^0 - \tau F_i) - \left(\tau^3 - \frac{3}{2} \tau^2 + \frac{7}{12} \tau - \frac{1}{24} \right) D^4 \hat{f}_i^0 + O(\epsilon^5) \\ = \frac{1}{\tau} (\hat{f}_i^0 - f_i), \end{aligned} \quad (40)$$

which is the extension of Eq. (25) to two more orders. Here the derivative operator is

$$D \equiv \partial_t + v_i \cdot \nabla. \quad (41)$$

For a stationary profile, advected with velocity U , we have the operator identity

$$\partial_t + U \cdot \nabla = 0. \quad (42)$$

This simplifies the derivative operator

$$D = (v_i - U) \cdot \nabla. \quad (43)$$

We now need to take the zeroth- and first-order moments of this expression to obtain the expressions for the continuity and Navier-Stokes level equations in the stationary advected limit. The expectation is that the continuity equation takes the form

$$\nabla \cdot (\rho \hat{u} - \rho U) = O(\epsilon^5), \quad (44)$$

and the Navier-Stokes level equation will become

$$\nabla \cdot (P) = O(\epsilon^5). \quad (45)$$

This then allows us to identify the effective mean fluid velocity \hat{u} to fifth order and the effective pressure tensor P also to fifth order. It is highly desirable, although far from obvious, that these quantities be independent of the relaxation

time τ . Otherwise, the equilibrium properties would be coupled to the transport coefficients.

This task is cumbersome since it involves up to fifth-order velocity moments of the equilibrium distribution function. We will restrict ourselves here to the analysis of a projection of the most common models (D2Q7, D2Q9, D3Q15, D3Q19, and D3Q27) to one dimension. This projection is the D1Q3 model, a one-dimensional model with three velocities. It is important to note that this analysis is entirely sufficient to determine the phase behavior of all the above models. The only issue not addressed by this analysis is the isotropy of the models. One caveat is that this analysis will only be able to make statements of the equilibrium behavior of the method, not about the approach to equilibrium.

A. Analysis of the D1Q3 model

The D1Q3 model is a one-dimensional lattice Boltzmann model with three velocities: $v_i = \{-1, 0, 1\}$. In this model there are only three distinct velocity moments at each lattice point, corresponding to the three densities f_i . The moments of the equilibrium density are

$$\begin{aligned} \sum_i (\hat{f}_i^0 + A_i) &= \rho, & \sum_i (\hat{f}_i^0 + A_i)v_i &= \rho u, \\ \sum_i \hat{f}_i^0 v_i^2 &= \rho u u + \frac{\rho}{3} + A. \end{aligned} \quad (46)$$

Because $v_i^3 = v_i, v_i^4 = v_i^2$, etc., all higher-order velocity moments are given by these first three moments. The three moments of the forcing term are given by

$$\sum_i F_i = 0, \quad \sum_i F_i v_i = F, \quad \sum_i F_i v_i^2 = 2Fu + \Psi. \quad (47)$$

The higher-order moments are similarly given by these first three moments.

The algebra involved in calculating the higher moments is quite extensive, so I will only outline the method here without giving lengthy intermediate results. Summing \sum_i , Eq. (40), gives an expression for the continuity involving all moments of \hat{f}_i^0 and F_i . Similarly we obtain such an expression containing all moments by summing \sum_i , Eq. (40), v_i to obtain the momentum equation. We can then use the momentum equation to express A in terms of the other moments and higher-order derivatives of A . Then we insert this expression repeatedly into itself [similarly to what we did for Eq. (24)] to express A completely in terms of the other moments and their derivatives.

This expression for A is then used to eliminate any A dependence in the continuity equation. We then use the resulting continuity equation to express u in terms of the other moments and higher-order derivatives of u . This expression for u is then inserted for all but the lowest-order derivatives of u of the continuity equation. The resulting continuity equation has the form

$$\nabla \left(\rho u - \frac{1}{2} F - \rho U \right) - \frac{1}{4} \nabla \nabla \left[F U + \frac{1}{3} \nabla (\rho U) \right] = O(\epsilon^5), \quad (48)$$

which only contains one term of u and no terms with A . We use this version of the continuity equation to express u in terms of U , ρ , and F and replace all occurrences of u in the momentum equation. We then remove all but the lowest-order occurrences of A in the momentum equation and obtain

$$\begin{aligned} F + \nabla \left[\frac{\rho}{3} + A - \left(\tau - \frac{1}{2} \right) [3FU + \nabla(\rho U)] + \frac{1}{4\rho} FF + \frac{1}{12} \nabla F \right. \\ \left. - \tau \left(\frac{FF}{\rho} + \Psi \right) \right] = O(\epsilon^5). \end{aligned} \quad (49)$$

Now we apply these results to our pressure and forcing methods.

B. Pressure method

For the pressure method we use the moments defined in Eq. (33) and obtain, for the continuity equation,

$$\nabla(\rho u - \rho U) - \nabla \nabla \left[\frac{1}{12} \nabla(\rho U) \right] = O(\epsilon^5). \quad (50)$$

Comparing this to Eq. (44) we see that the mean fluid velocity is

$$\hat{u} = \frac{u}{1 + \frac{1}{12} \frac{\nabla^2 \rho}{\rho}}. \quad (51)$$

The gradient term is a new correction for the measurement of the velocity for the pressure method. For the momentum equation we obtain

$$\nabla P = O(\epsilon^5). \quad (52)$$

There are no additional pressure terms for the pressure method, which is consistent with the fact that we found a constant input pressure for simulations with the pressure method in Figs. 1(b) and 2(b).

To test the correction for the velocity predicted in Eq. (51) we have to consider a situation in which U is not zero. We set up a profile that is initiated with a velocity of $U=0.01$. In Fig. 4(a) we plot both the standard velocity u from Eq. (9) and our approximation of the true fluid velocity \hat{u} from Eq. (51). First we note that the gas phase is advected faster than the liquid phase, which is a problem of Galilean invariance [15]. The gas is advected faster than the liquid, and a constant evaporation on the leading edge of the droplet and a condensation at the trailing interface of the liquid lead to a mean interface velocity that is less than the imposed mean fluid velocity of 0.01. This evaporation and condensation lead to an additional velocity ξ of the interface. For such an interface velocity we have an additional contribution to the change of the density, the rate of evaporation given by

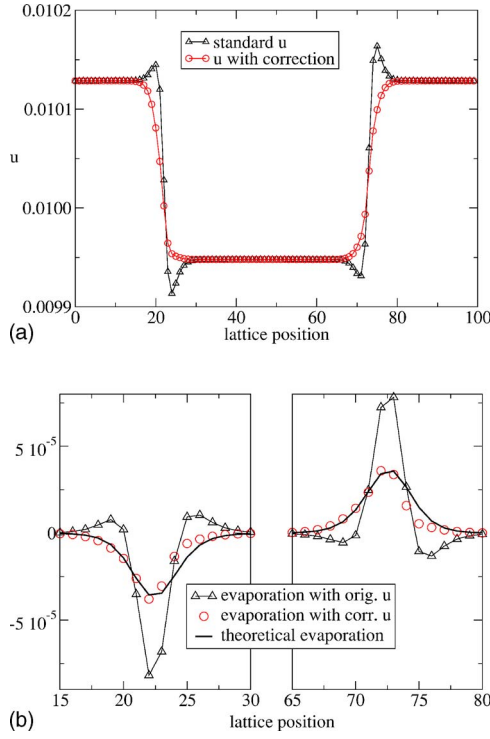


FIG. 4. (Color online) Comparison of the expression for the mean fluid velocity from original definition (9) and the corrected version (51) for the pressure method in (a). The system was initialized with a constant velocity of $U=0.01$. While the correction term clearly removes some spurious velocity terms, there is a more noticeable violation of Galilean invariance which advects the gas phase faster than the liquid phase with respect to the lattice. In (b) we compare the measured expression for the evaporation $\nabla[\rho(U - \hat{u})]$ for the original and corrected expressions for \hat{u} and compare it with the theoretical one of $\xi \nabla \rho$ for $\xi = -0.0002$. This simulation was performed with $\theta_c = 0.35$, $\theta = 1/3$, and $\kappa = 0.1$.

$$(\partial_t + U \cdot \nabla)\rho = -\xi \cdot \nabla \rho = \nabla[\rho(U - \hat{u})]. \quad (53)$$

So to compare the original definition of \hat{u} from Eq. (27) with the corrected definition of Eq. (51) we plot $\nabla[\rho(\hat{u} - U)]$ for the two definitions of \hat{u} and $\xi \nabla \rho$ in Fig. 4(b). We see that the corrected version of the velocity allows a very good fit with the theoretical expression. The best fit for ξ is -0.0002 which corresponds to a 2% correction for the observed domain velocity.

While the Galilean invariance violations are small, in this case it is still worthwhile to correct the Galilean invariance violations of the lattice Boltzmann method. To do that we need an expansion that does not make the assumption $u = O(\epsilon)$. This investigation of higher-order Galilean invariance violations will be reported elsewhere.

C. Forcing method

For the forcing method (32) we obtain the continuity equation

$$\nabla \left(\rho u - \frac{1}{2} F - U \right) = O(\epsilon^5). \quad (54)$$

This implies that the mean fluid velocity is given by $\hat{u} = \rho u - F/2$, in agreement with the lower-order expression (27).

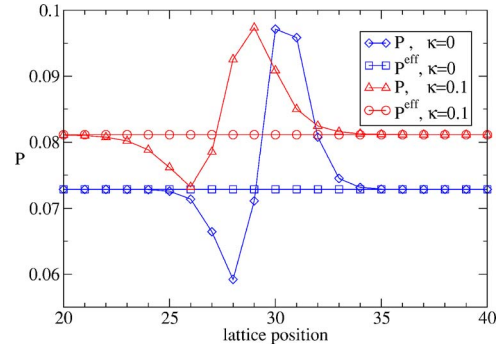


FIG. 5. (Color online) Comparison of the input pressure P from Eq. (37) and the effective pressure P^{eff} of Eq. (57) for the forcing method for two values of κ . We see that the effective pressure P^{eff} is constant to machine accuracy in both cases. This agreement is better than expected since expansion predicted this pressure only up to fifth order. The critical temperature for this simulation is $\theta_c = 0.37$ at $\theta = 1/3$ so that the true equilibrium pressure is 0.09.

There are no further corrections to the velocity for the forcing method to this level of approximation.

To evaluate the higher-order terms for the pressure in Eq. (49) we need to insert the specific form of the force. We have

$$\rho F = \nabla^D P^{nid} = \sum_{k=0}^{\infty} \frac{\nabla^{2k+1}}{(2k+1)!} P^{nid}. \quad (55)$$

With this expression for F the momentum equation becomes

$$\nabla \left[P - \left(\tau - \frac{1}{4} \right) \frac{FF}{\rho} + \frac{1}{4} \nabla^2 F \right] = O(\epsilon^5), \quad (56)$$

where we have again expressed some of the higher-order contributions in terms of the force. We conclude that the effective pressure is given by

$$P^{eff} = P - \left(\tau - \frac{1}{4} \right) \frac{FF}{\rho} + \frac{1}{4} \nabla^2 F + O(\epsilon^4). \quad (57)$$

This explains why the input pressure is not constant for the current forcing method. To verify this analytical result we can plot both the input pressure P and the predicted effective pressure P^{eff} for a phase-separated stationary profile obtained from the forcing version of the lattice Boltzmann simulation. The result is shown in Fig. 5.

Somewhat surprisingly, the pressure P^{eff} is not simply a fifth-order approximation to the true pressure. Instead, for $U=0$, this gives a pressure that is constant to machine accuracy. To be exact what is constant is the discretization

$$P^{eff} = P - \left(\tau - \frac{1}{4} \right) \frac{FF}{\rho} + \frac{1}{4} \nabla^{2(D)} P - \frac{1}{12} \nabla^{2(D)} \rho. \quad (58)$$

This is, presumably, due to the fact that the higher-order moments are just repeats of the lower-order moments and this allows the higher-order moments to consist of higher-order derivatives of the lower-order moments. Unfortunately this exact solution no longer holds if $U \neq 0$, because the higher-order moments contain higher powers of U . The fact that we know an *exact* pressure that we minimize may prove

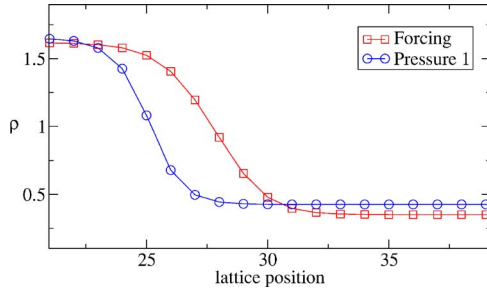


FIG. 6. (Color online) The performance of the corrected forcing method gives results that are identical to the results of the pressure method. The interfaces correspond exactly. Therefore the pressures and the chemical potentials also agree. Simulation parameters are $\theta_c=0.37$, $\theta=1/3$, and $\kappa=0.1$.

to be very useful for diffusive systems, though, for which we have $U=0$.

This may also open the door for an important application of mimetic calculus. If we were able to find some discrete gradient operators ∇^δ for which $\nabla^\delta P = \rho \nabla^\delta \mu$ holds, we would be able to devise a method that *always* recovers the correct equilibrium behavior.

D. Forcing method

Now that we have identified the effective pressure P^{eff} that is constant in the steady state we can identify a method that will have a constant input pressure P . Investigating Eqs. (48) and (49) we can identify a choice of Ψ that will allow us to cancel the additional pressure terms due to the force. We can amend the original forcing method (32) with

$$\tau\Psi = \left(\tau - \frac{1}{4}\right)\frac{FF}{\rho} + \frac{1}{12}(\nabla\nabla)^D\rho. \quad (59)$$

We then obtain the continuity equation

$$\nabla\left(\rho u - \frac{1}{2}F - U\right) = O(\epsilon^5) \quad (60)$$

and the momentum equation

$$\nabla P = O(\epsilon^5). \quad (61)$$

The choice of Ψ is not unique regarding the exact choice of the correction terms. We could replace $(\nabla\nabla)^D\rho$ with $-3\nabla^D F$ and still remain correct up to $O(\epsilon^5)$. However, the above choice again leads to a pressure that is constant up to machine accuracy for $U=0$, just as we did with the pressure method.

A comparison of the pressure method and the corrected forcing method is shown in Fig. 6. The new forcing method is nearly indistinguishable from the pressure method. One small difference between the two methods is that an alternating pattern in the pressure does not lead to a force and, therefore, does not decay. In the simulation shown in Fig. 6 those pressure oscillations have an amplitude of about 10^{-5} . However, in some simulations these oscillations can become large. Also for large velocities these oscillations can become unstable and make this method less stable than the pressure method at large velocities.

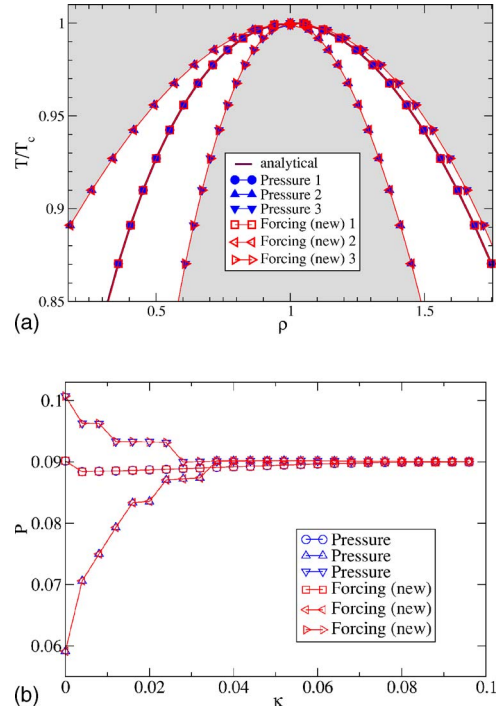


FIG. 7. (Color online) The pressure and the new forcing methods give equivalent results. We see that the phase diagram for $\kappa=0$ even reproduces the nonuniqueness of the solutions. The recovery of a universal profile also occurs at the same pace in the forcing and pressure methods derived in this paper, as shown in (b).

Because the pressure and chemical potential depend only on the profile $\rho(x)$ the new forcing method gives the same constant pressure and near-constant chemical potential as the pressure method shown in Fig. 2. This forcing method is therefore thermodynamically consistent. It also recovers the analytical phase diagram, as shown in Fig. 8, below.

We also examined the behavior of the forcing method in the limit where $\kappa \rightarrow 0$. This limit may appear tricky because the correction terms need to cancel the numerical derivatives we uncovered in the expansion. This should uncover any higher-order terms that we missed in our expansion. We find, however, that the method described here will even recover the sharp interfaces we observed for the pressure method. The nonuniqueness of the solutions which we found for the pressure method is also observed for the pressure method. The recovery of a unique solution for larger values of κ occurs at the same pace as for the pressure method. This is shown in Fig. 7. This surprising result is due to the fact that the pressure P is exactly constant for both methods.

VI. DISCUSSION

In this paper we have shown that forcing terms lead to non-negligible higher-order terms for systems with large density gradients. We introduced an equilibrium analysis method, which allowed us to identify correction terms up to fifth order. This equilibrium analysis allowed us to identify those correction terms. This analysis gave the exact pressure for systems that are not advected with respect to the lattice.

Correction terms similar to, but different from, the correction terms we identified have been proposed by Guo *et al.* [16]. Their analysis leads them to conclude that for a body force we should choose (in the notation of this paper)

$$\tau\Psi = \left(\tau - \frac{1}{2}\right)\rho FF. \quad (62)$$

Comparing this to Eq. (59) we find that this term is different in that we predict a factor of 1/4 instead of 1/2 as well as an additional double-derivative term of ρ . The correction term (62) was derived using a multiscale analysis to second order. We did not understand how these terms could be consistently derived with a second-order expansion. In a Taylor expansion the term $\nabla(\rho FF)$ appears only as a third-order term. It is likely that a second-order expansion would not pick up the $\nabla\nabla^2\rho$ term. If this expansion can pick up the ρFF term in Ψ consistently, however, there cannot be a difference in the prefactor of this term when it is derived by a Taylor expansion method.

It is therefore important to compare the correction term predicted in [16] to our correction term Ψ of Eq. (59). We implemented the correction term (62). We then performed simulations with pressure (36) which does not include interfacial terms. We would therefore expect a sharp interface. We do, however, observe that this method leads to an extended interface, indicating that there are additional gradient terms in the pressure not accounted for by the Navier-Stokes equation derived by Guo *et al.* [[16], Eq. 18b]

We also measured the phase diagram for the original forcing method, the corrections proposed by Guo, and the new forcing method. The results are shown in Fig. 8. We see that the correction introduced by Guo *et al.* improves the result for the forcing method somewhat. However, there is still no good agreement with the theoretical phase diagram. This is, however, achieved by the correction derived in this paper when we include additional gradient terms in the pressure tensor (37). This suggests that the prefactor derived in the current work is correct.

There is a long-standing discussion about the suitability of pressure methods for the simulation of nonideal fluids [8,10]. The criticism relies on the general argument that there should be a close correspondence between the lattice Boltzmann equation and kinetic theory. At this level it is a somewhat philosophical argument. And this philosophical argument is weakened by the occurrence of lattice correction terms that have no analogy in kinetic theory. A more useful test should be the ability of the forcing and pressure methods to recover

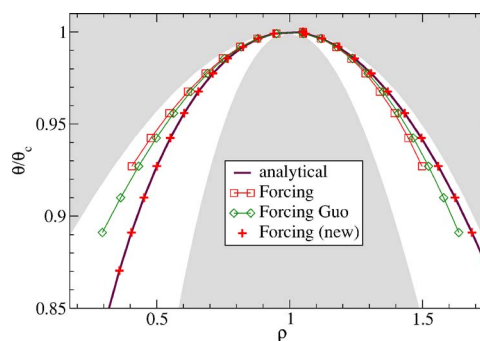


FIG. 8. (Color online) Comparison of the effect of correction terms to the forcing method derived by Guo *et al.* [16] and the current paper. We use the pressure of Eq. (36). We observe that the agreement with the phase diagram is improved using the correction terms from [16]. For the forcing method derived in the current paper the results would be indeterminate just at the results of the pressure method in Fig. 1. However, including gradient terms of Eq. (37) with $\kappa=0.1$ we recover thermodynamic consistency.

correct solutions in a robust and stable manner. As far as the recovery of equilibrium solutions is concerned, we find that there is no fundamental difference in the suitability of including nonlinear pressure terms into a lattice Boltzmann method through a forcing term or a pressure term.

As a next step in this analysis we need to compare the performance of the different methods under Galilean transformations. To uncover any terms that have not been previously discussed [15] requires us to drop the assumption of small velocities in our fifth-order expansion. Those results will be published elsewhere.

To truly distinguish between the two approaches, however, the analysis of dynamic solutions is required. There are very few tests in the literature of nonstationary solution for liquid-gas lattice Boltzmann simulations. But such tests will be required to compare the differences between pressure and forcing approaches. Examples of such simulations include advected fluids undergoing phase separations. For density small compared to the equilibrium densities analytical solutions exist for $\rho(x,t)$.

In closing we want to point out that the corrections for the forcing method for phase-separated systems do also apply for external forces. The same additional pressure terms that we identified in Eq. (58) also occur when a truly external force acts on the system. This is particularly important to keep in mind when simulating liquid-gas systems in the presence of gravity.

[1] A. K. Gunstensen, D. H. Rothman, S. Zaleski, and G. Zanetti, Phys. Rev. A **43**, 4320 (1991).
 [2] X. Shan and H. Chen, Phys. Rev. E **49**, 2941 (1994).
 [3] M. R. Swift, E. Orlandini, W. R. Osborn, and J. M. Yeomans, Phys. Rev. E **54**, 5041 (1996).
 [4] Y. Chen, S. Teng, T. Shukawa, and H. Ohashi, Int. J. Mod. Phys. B **9**, 1383 (1998).

[5] E. Aurell and M. Do-Quang, cond-mat/0105372.
 [6] Most textbooks on thermodynamics—e.g., H. B. Callen, *Thermodynamics and an Introduction to Thermostatistics* (Wiley, New York, 1985).
 [7] X. Y. He, X. W. Shan, and G. D. Doolen, Phys. Rev. E **57**, R13 (1998).
 [8] X. He and G. D. Doolen, J. Stat. Phys. **107**, 309 (2002).

- [9] D. J. Holdych, D. Rovas, J. G. Georgiadis, and R. O. Buckius, *Int. J. Mod. Phys. C* **9**, 1393 (1998).
- [10] L-S. Luo, *Phys. Rev. Lett.* **81**, 1618 (1998).
- [11] A. J. Wagner, Ph.D. thesis, Oxford University, 1997.
- [12] A. J. Wagner and J. M. Yeomans, *Int. J. Mod. Phys. C* **9**, 1373 (1998).
- [13] S. Ansumali and I. V. Karlin, *Phys. Rev. Lett.* **95**, 260605 (2005).
- [14] After an initial discussion about this subject most experts now appear to agree that, at least to second order, the two approaches
- agree. However, I was unable to find a detailed comparison of the two approaches in the literature.
- [15] A. J. Wagner and Q. Li, *Physica A* **362**, 105 (2005).
- [16] Z. Guo, C. Zheng, and B. Shi, *Phys. Rev. E* **65**, 046308 (2002).
- [17] T. Inamuro, N. Konishi, and F. Ogino, *Comput. Phys. Commun.* **129**, 32 (2000).
- [18] A. N. Kalarakis, V. N. Burganos, and A. C. Payatakes, *Phys. Rev. E* **65**, 056702 (2002).